Respiration

Clinical Investigations

Respiration 2023;102:274–286
DOI: 10.1159/000529388

Received: June 2, 2022
Accepted: January 6, 2023
Published online: February 7, 2023

Subject-Specific Activation of Central Respiratory Centers during Breath-Holding Functional Magnetic Resonance Imaging

Carolina Ciumas[a, b, c] Mayara Bolay[a] Romain Bouet[d] Sylvain Rheims[b, c, e] Danielle Ibarrola[f] Johnson P. Hampson[g] Samden D. Lhatoo[g] Philippe Ryvlin[a]

[a]Department of Clinical Neurosciences, Lausanne University Hospital and University of Lausanne, Lausanne, Switzerland; [b]Lyon Neuroscience Research Center, Institut National de la Santé et de la Recherche Médicale U1028/CNRS UMR 5292 Lyon 1 University, Bron, France; [c]IDEE Epilepsy Institute, Lyon, France; [d]Eduwell team, Lyon Neuroscience Research Center (CRNL), Inserm U1028, CNRS UMR5292, UCBL1, UJM, Lyon, France; [e]Department of Functional Neurology and Epileptology, Hospices Civils de Lyon, Lyon, France; [f]Cermep - Imagerie du vivant, CNRS UAR, Bron, France; [g]Department of Neurology, McGovern Medical School, University of Texas Health Science Center at Houston, Houston, TX, USA

Keywords
Brainstem · Respiratory control · Breath-holding · Healthy volunteers · Functional magnetic resonance imaging

Abstract
Background: Voluntary breath-holding (BH) triggers responses from central neural control and respiratory centers in order to restore breathing. Such responses can be observed using functional MRI (fMRI). ***Objectives:*** We used this paradigm in healthy volunteers with the view to develop a biomarker that could be used to investigate disorders of the central control of breathing at the individual patient level. ***Method:*** In 21 healthy human subjects (mean age±SD, 32.8 ± 9.9 years old), fMRI was used to determine, at both the individual and group levels, the physiological neural response to expiratory and inspiratory voluntary apneas, within respiratory control centers in the brain and brainstem. ***Results:*** Group analysis showed that expiratory BH, but not inspiratory BH, triggered activation of the pontine respiratory group and raphe nuclei at the group level, with a significant relationship between the levels of activation and drop in SpO_2. Using predefined ROIs, expiratory BH, and to a lesser extent, inspiratory BH were associated with activation of most respiratory centers. The right ventrolateral nucleus of the thalamus, right pre-Bötzinger complex, right VRG, right nucleus ambiguus, and left Kölliker-Fuse-parabrachial complex were only activated during inspiratory BH. Individual analysis identified activations of cortical/subcortical and brainstem structures related to respiratory control in 19 out of 21 subjects. ***Conclusion:*** Our study shows that BH paradigm allows to reliably trigger fMRI response from brainstem and cortical areas involved in respiratory control at the individual level, suggesting that it might serve as a clinically relevant biomarker to investigate conditions associated with an altered central control of respiration.

Carolina Ciumas and Mayara Bolay are co-first authors.

Karger@karger.com
www.karger.com/res

Correspondence to:
Carolina Ciumas, carolina.ciumas@gmail.com

Introduction

Physiological rhythmic breathing in humans depends on the activity of several brainstem nuclei, including the ventral respiratory group or column (VRG or VRC), dorsal respiratory group (DRG), and nucleus ambiguus (NA) in the medulla oblongata, and pontine respiratory group (PRG) composed of the pneumotaxic center (Kölliker-Fuse/parabrachial complex) with tight connection to the locus coeruleus (LC) and apneustic center [1]. Cortical and subcortical structures are also involved in respiratory control, with the amygdala and frontal cortex, including the cingulate, mediating the affective component of breathing, while the somatosensory cortex and dorsal striatum are involved in the motor control of respiration [2].

Dysfunctions of respiratory centers are likely to occur in several conditions, including obstructive sleep apnea (OSA) [3], sudden unexpected death in epilepsy patients (SUDEP) [4], sudden infant death syndrome [5], Prader-Willi syndrome [6], and congenital central hypoventilation syndrome (Ondine's syndrome) [7]. Yet, while a number of studies have explored the physiological mechanisms of breathing, such as distribution of respiratory centers in the brainstem or central regulation during hypercapnic challenges in rats [8–10], little is known about the changes in the human brain and brainstem control of respiration in these conditions. A better understanding of the central respiratory function and dysfunctions in humans could help develop clinically relevant biomarkers and interventions, with the view to predict and prevent tragic outcomes, such as SUDEP.

Functional magnetic resonance imaging (fMRI) offers opportunities to investigate this issue using a simple voluntary breath-holding (BH) paradigm which can be implemented in any MRI setting and readily translated into clinical practice if proved useful. Central respiratory activity continues throughout BH which triggers responses from respiratory centers, including suppression of pacemaker cell activity in the VRG [11]. Previous fMRI BH studies in small cohort of healthy subjects showed promising findings in a small sample, with significant brainstem and cortical/subcortical responses [12, 13]. BH does not require any specialized equipment and is rather simple to employ in clinical settings. Previous research suggested that this strategy produced a reliable fMRI BOLD response similar to that triggered by hypercapnia produced by controlled CO_2 inhalation [14–18]. These studies identified a variety of anatomical and physiological mechanisms behind the generation and modulation of respiratory rhythm as well as the selective engagement of brainstem respiratory centers in BH control [13, 19]. We further detailed these findings in a very recent review [20] and observed that little information was available as to which type of BH produces the stronger central response or whether the response is identical with inspiratory or expiratory BH. In this study, we aimed at further exploring BH-triggered fMRI activation of brain and brainstem respiratory centers with the view to test the possibility to delineate reliable BOLD responses at the individual level in healthy subjects. Such individual responses would be a prerequisite for the development of fMRI biomarkers for patients with respiratory dysfunction of central origin.

Materials and Methods

Subjects

Healthy volunteers aged 18–55 years old were recruited through advertisement. Exclusion criteria included (1) ongoing or chronic medical conditions, (2) history of respiratory or neurological disease, (3) intake of medication except oral contraceptives, (4) pregnant women, (5) subjects living at high altitude (>2,000 m), (6) subjects practicing free-diving, (7) any contraindication to an MRI investigation. All subjects gave their written informed consent to participate in the study which was approved by the Ethics Committee of Canton de Vaud.

Physiological Signals

Before starting the MRI session, subjects were equipped with MRI-compatible materials that provided permanent measurements of respiratory movements using a respiration transducer (Biopac Systems Inc., Goleta, CA, USA), pulse oximetry using a finger transducer (Nonin Medical, Plymouth, MN), and a mouthpiece with a cannula to measure end-tidal O_2 and CO_2 (Biopac Systems Inc.).

Behavioral Experiment

The experimental procedure was explained in detail to all subjects prior to their participation. Participants were trained to restrict any head and neck movements during the whole experiment. All participants were visually observed and guided during the initial training period to ensure they fully comply with the instructions to minimize movements after BHs, in particular forced gasping.

Participants were pseudo-randomly assigned to start the fMRI experiment with either the inspiratory or expiratory BH task. The experiment was divided into a resting part and a functional part and lasted on average 60 min during which physiological respiratory data were continuously recorded. In the first 20 min, subjects breathed normally while structural MR images were acquired. This also enabled subjects to adapt to breathing in the MRI gantry in order to ensure stable and regular breathing during the baseline parts of the fMRI experiment.

During the fMRI part, each subject performed four BH runs, including two inspiratory and two expiratory, with six blocks of BH within each run (Fig. 1). Each run lasted between 7 and 11 min

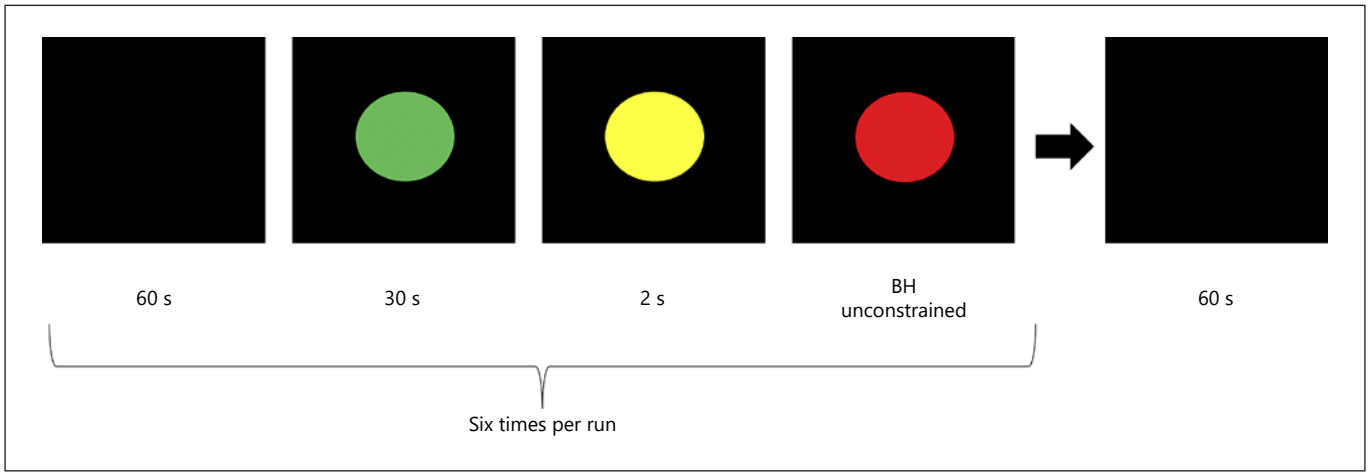

Fig. 1. Example of one of the six blocks in a run (expiratory or inspiratory). Subjects performed four runs (two inspiratory unconstrained BH runs and two expiratory unconstrained BH runs).

depending on the individual's capacity to fulfill the task. Given the previous observation that BOLD signal variability during BH can be significantly reduced with the use of visually cued tasks [21], we used colored circle instructions on the screen as illustrated in Figure 1. A dedicated workstation running Presentation software (Neurobehavioral Systems, San Francisco, CA, USA) was used to control the presentation of cues and record subjects' responses. A green dot was first presented on the screen for 30 s during which the subject was instructed to breathe normally through the mouthpiece; then, a 2-s duration yellow dot was shown, indicating that the subject needed to prepare himself for an expiratory or inspiratory BH that shall start at the end of an expiration or inspiration, respectively, and at the end of the 2 s. Finally, a red dot was displayed to indicate the onset and continuation of BH as long as the subject could handle it while keeping comfortable. Subjects pushed a button at the time they resumed breathing, which turned the dot green again.

MRI Imaging and Protocol

Participants were examined on a 3T whole-body MRI system (Magnetom Prisma, Siemens Medical Systems, Germany), using a 64-channel RF receiver head coil and body coil for transmission. The structural MRI protocol included 10 min of anatomical imaging (sagittal MPRAGE, slice tilt = 8°, echo time, 2.67 ms; repetition time, 3.50 s; TI = 1,000 ms, matrix size = 256, field of view = 224 mm, slice thickness = 0.9 mm, voxel size 0.9 × 0.9 × 0.9 mm) followed by 6-min time of flight imaging (slice tilt = 18°, echo time, 3.43 ms; repetition time, 0.21 s; slice thickness = 0.6 mm, GRAPPA factor 2) to acquire vascular structures, in particular that of vertebrobasilar arteries. These were used to ensure that BOLD signal changes acquired during the fMRI experiment were deemed located in the brainstem parenchyma and not reflecting spill-over effect from changes occurring in nearby vessels.

The fMRI protocol used a gradient-echo T2*-weighted echo-planar imaging sequence as described in the study by Beissner et al. 2014 [22] (slice tilt = 40°, echo time, 30 ms; repetition time, 2.52 s; slice thickness = 2.5 mm, GRAPPA factor 2) covering the whole brain, including the lower brainstem. The proposed protocol is based on experiments previously published in the field and which proved effective at investigating brain and brainstem BOLD response [12, 21].

Data Preprocessing

Times of onset, termination, and duration of each BH were determined by using several sources of information: (1) those that were automatically recorded through the Presentation software which provided the theoretical times of BH onset (red cue) and termination (button pressed by the subject), and (2) the recorded respiratory movements whose peaks were automatically identified by an in-house MATLAB-based software. As a rule, these sources of information were highly concordant, while in a few subjects, BH was slightly delayed following the red cue or terminated slightly prior to pressing the button. We also inspected the evolution of end-tidal CO_2 and O_2 during BH to ensure lack of inconsistency. BH blocks associated with variations in gas concentration and thoracic movements were discarded from the analysis. Apnea events were defined in this study as cessation of airflow for more than 10 s. Whenever BH was associated with a drop in SpO_2 ≥4% from baseline, which is considered clinically significant [23], we marked the decline between the onset and offset of the SpO_2 drop.

We tested the similarity of the apnea duration values automatically obtained from the recording system to those corrected manually, using a correlation coefficient. The difference in drop of SpO_2 between inspiratory and expiratory BH was assessed for homogeneity (Levene's test) and compared between conditions using a Mann-Whitney U test. The duration of apnea reported by subjects highly correlated with that measured through objective respiratory movements (correlation coefficient, $R = 0.963$ for expiratory BH, $R = 0.954$ for inspiratory BH) (see Table 1).

fMRI studies of the human brainstem have proved challenging for various methodological reasons [24]. BH maneuver is accompanied by changes in breathing rate and depth across the various phases of the experiment, which cause significant and faster respiration-induced BOLD-like signal fluctuations that need to be fil-

Table 1. Apnea during BH

	Expiration	Inspiration
Median apnea duration in s (range)	28.4 (16.9–53.5)	44.7 (26.6–67.4)
Subjects with duration of apnea <20 s, *n* (%)	2 (9.5)	0
Subjects with duration of apnea between 20 and 30 s, *n* (%)	10 (47.6)	4 (19)
Subjects with duration of apnea between 30 and 40 s, *n* (%)	8 (38.1)	6 (28.6)
Subjects with duration of apnea >40 s, *n* (%)	1 (4.8)	11 (52.4)

Table contains dispersion of mean duration of apnea per BH type for each subject.

tered [25, 26]. BH also alters the levels of O_2 and CO_2, thus inducing mild hypoxia and increased hypercapnia, which directly influence the BOLD contrast [27]. Finally, cardiac-related artifacts are arising from brain movement caused by fluctuating blood pressure and blood volume during each heart beat [28]. Delineating the temporal dynamics of these susceptibility-induced changes is thus required to measure the true BOLD signal changes occurring in the brain and brainstem respiratory centers and reduce the risk of false-positive and false-negative findings [27, 29, 30]. To this end, end-tidal CO_2 was convolved with the response function and regressed out of the BOLD signal at each voxel, producing the corrected data. The subject-specific end-tidal CO_2 was calculated from the points of maximum CO_2 values at the end of each exhale, linearly interpolating between them, and resampling the result to the TR timing (2,520 ms). For BH periods in which there were no end-tidal CO_2 values, the interpolation range was between the last exhale before BH and the first after, as described previously [31]. The detection of the "respiration and circulation response function" was accomplished by incorporating the measurement of thoracic breathing movements and cardiac heartbeats into the model [22, 25, 32].

MRI data were processed using MATLAB 7.6 (Mathworks Inc., Sherborn, MA, USA) with statistical parametric mapping software (SPM12, Wellcome Department of Imaging Neuroscience, London, UK). The first four volumes were discarded to allow the MRI signal to reach equilibrium. All images were then realigned to the mean functional image, which was co-registered with the anatomical image. The T1 volume was segmented by DARTEL. The deformation maps were applied to the realigned functional volumes for spatial normalization and the volume resliced to $2 \times 2 \times 2$ mm voxels in MNI space. Normalized volumes were then smoothed at 4 mm full-width half-maximum.

Our primary endpoint was the BOLD activation measured in brainstem respiratory centers following inspiratory and expiratory BH as compared to baseline, at both the individual and group levels. According to this specific objective and in order to increase statistical power, we created and used a mask of the brainstem and cortical/subcortical areas known to participate in breathing control. This mask was built using the regions of interest (ROIs) derived from "Hammersmith atlas n30r83" atlas [2, 33–35]. Brain structures described in the literature as playing a significant role in the regulation of breathing during apnea and selected for the mask included the prefrontal cortex [2, 36, 37], pre- and postcentral gyrus [33, 36, 37], thalamic nuclei (ventrolateral nucleus [VL], anterior nucleus [ANT]) [33, 36, 37], hypothalamus [33, 36, 37], insula, hippocampus [2, 33–35], amygdala [2, 33–35], and anterior cingulate [2, 33–35].

Because the brainstem structures involved in respiratory control are fairly small, besides looking at the signal change in the whole structure, we also opted for individual ROIs to observe their response during our experiment. Spherical ROIs (diameter = 3 mm) were placed in the volumetric center of respiratory centers in the brainstem and subcortical nuclei involved in breathing control. The ROI location was adjusted to include only gray matter voxels and limit any overlapping voxels when possible. The coordinates of the circular ROIs of the brainstem and subcortical structures are listed in Table 2. Their location was identified either by validating their location in human brain atlases, if available, or identifying their position according to described landmarks (refer to Table 2).

Statistics

SPM analyses of preprocessed MRI data were performed using a general linear model. We created several contrasts to identify a significant difference once comparing two variables to one another. General linear model included inspiratory BH, expiratory BH, SpO_2 falls and rises during inspiratory and expiratory BH, and deactivations during BH. Contrasts of interest were generated by comparing the beta weights associated with BOLD activation in response to BH. Cluster corrected significance level was set at $p < 0.05$ after family-wise error correction for multiple comparisons for the number of voxels tested for the group analyses and individual subject responses (for visualization purpose, figures also show clusters at $p = 0.001$). BOLD activation maps from each individual subject were also compared to those from the group composed of all other subjects with the view to test whether some normal subjects would significantly differ from the others. Ideally, one would hope not to detect significant findings in subjects without respiratory disorder but only in patients with such disorders.

ROI-based analyses of the mean % change in BOLD signal in brainstem and diencephalon respiratory centers were performed using a multivariate statistic (MANOVA) and post hoc non-parametric tests (LSD) for every individual ROI ($p < 0.05$). We compared the mean β value of each ROI, during the expiratory BH, inspiratory BH, and baseline. We assessed the percentage of subjects presenting a BOLD signal change in the brainstem and investigated the relation between such changes and the duration of apnea and drop in SpO_2.

Table 2. Coordinates of circular ROIs selected based on the literature

Structures	Location	Left	Right
ANT of the thalamus [2]	Gray matter, dorsal part of the diencephalon	−6; −6; 4	8; −6; 4
VL of the thalamus [2]		−10; −14; 4	14; −14; 4
LC [5, 2]	Posterior area of the rostral pons in the lateral floor of the fourth ventricle	−3; −32; −24	7; −32; −24
Kölliker Ffuse-PB complex [5, 2]	Bilateral, rostral dorsolateral pons	5; −30; −24	−4; −30; −24
DRG of the nucleus tractus solitarus [31, 32]	Ventral-lateral portion of the tractus solitarus	−4; −38; −52	6; −38; −52
NA [32]	Ventrolateral medullary reticular formation	−4; −32; −52	6; −32; −52
PBC [9, 28]	Ventrolateral medullary reticular formation at the rostrocaudal level +9 mm from obex	−4; −32; −52	4; −32; −52
VRG [31]	Bilateral column, lateral tegmentum. From caudal part of facial nucleus to C1 spinal level	−4; −36; −52	−6; −36; −52
Lateral reticular nucleus [2]	Medulla Oblongata, caudal ventrolateral	−5; −36; −52	6; −36; −52
Dorsal raphe nucleus [32]	Medial portion of the reticular formation	2; −25; −12	
Median raphe nucleus [32]			1; −28; −18

The coordinates on the right represent the center of mass, and each ROI is made up of a sphere formed around this center of mass.

Table 3. Descriptive data

Controls	Sex	Age, years	Weight, kg	Height, cm	Height, m	BMI, kg/m^2
1	Male	37	90	179	1.79	28.1
2	Female	23	63	173	1.73	21.0
3[a]	Female	43	69	155	1.55	28.7
4	Male	32	66	182	1.82	19.9
5	Male	48	90	181	181	27.5
6[a]	Male	27	67	171	1.71	22.9
7[a]	Female	22	51	172	1.72	17.2
8	Female	46	64	153	1.53	27.3
9	Male	32	78	177	1.77	24.9
10[a]	Male	31	70	187	1.87	20.0
11	Female	20	60	168	1.68	21.3
12	Female	29	55	161	1.61	21.2
13	Female	26	44	155	1.55	18.3
14	Female	22	64	163	1.63	24.1
15	Male	53	54	173	1.73	18.0
16[a]	Male	24	73	184	1.84	21.6
17	Female	27	54	159	1.59	21.4
18	Male	38	78	180	1.8	24.1
19	Female	32	57	170	1.7	19.7
20	Male	27	80	178	1.78	25.2
21	Female	49	60	174	1.74	19.8

Two of the participants were underweight (BMI <18.5 kg/m^2), 14 had a normal weight (BMI between 18.5 and 24.9 kg/m^2), five were overweight (BMI between 25 and 29.9 kg/m^2), and none were obese (BMI >30 kg/m^2). [a] Subjects practiced high-intensity physical trainings on a regular basis.

Results

Subjects Characteristics

We included 21 healthy subjects in the study (52.4% females, 47.6% males), with a mean age ± SD of 32.8 ± 9.9 years, Table 3. No subject was excluded from the study.

Behavioral Response

We observed a great inter-individual heterogeneity in the duration of apneas, which lasted longer for inspiratory BH (median 44.7 s, range 26.6–67.4 s) than for expiratory BH (median 28.4 s, range 16.9–53.5 s). During expiratory BH, two of the 21 subjects (9.5%) achieved a

Table 4. General linear model group analyses

Hemisphere Expiratory BH	Lobe	Structure	*p* (FWE correction)	Cluster size, voxels	T	*Z* score	*x*	*y*	*z*, mm
Left	Limbic	Parahippocampal gyrus	0.000	7	10.51	5.97	−12	−31	−4
		Hippocampus			6.51	4.67	−18	−25	−7
Left	Sublobar	Caudate	0.000	4	9.54	5.71	−12	−4	14
Left	Frontal	Inferior frontal gyrus	0.012	1	8.12	5.27	−45	14	−7
Left	Limbic	Parahippocampal gyrus	0.000	6	7.82	5.17	−21	−1	−13
Left cerebellum	Anterior	Culmen	0.012	1	7.24	4.96	−12	−28	−22
Right	Sublobar	Thalamus	0.001	3	7.00	4.87	15	−16	8
Right	Sublobar	Caudate	0.012	1	6.74	4.76	12	−4	14
Midline	Brainstem	Pons	0.000	4	6.72	4.75	0	−16	−19
Right	Frontal	Precentral gyrus	0.000	4	6.62	4.71	51	−7	29
Left cerebellum	Anterior	Culmen	0.012	1	6.56	4.69	−18	−28	−28
Right	Limbic	Parahippocampal gyrus	0.000	4	6.35	4.59	24	2	−13
Right	Sublobar	Thalamus	0.003	2	6.20	4.53	6	−28	−1
Right	Limbic	Parahippocampal gyrus	0.003	2	6.18	4.52	15	−31	−4
Right	Sublobar	Insula	0.003	2	6.09	4.48	39	−19	2
Right	Frontal	Precentral gyrus	0.012	1	6.01	4.44	51	−10	38
Inspiratory BH									
Left	Sublobar	Caudate	0.001	3	11.17	6.13	−12	−4	14
Right	Frontal	Precentral gyrus	0.000	8	9.09	5.58	51	−7	26
Left	Parietal	Postcentral gyrus	0.000	7	8.12	5.27	−36	−19	44
Right	Sublobar	Thalamus	0.000	4	7.61	5.10	9	−13	11
Right	Frontal	Medial frontal gyrus	0.001	3	7.57	5.08	3	29	38
Right	Sublobar	Caudate	0.010	1	7.30	4.98	12	−4	14
Left	Frontal	Precentral gyrus	0.000	6	7.25	4.96	−54	−10	38
Right	Frontal	Precentral gyrus	0.010	1	7.04	4.88	48	−10	38
Left	Frontal	Inferior frontal gyrus	0.001	3	6.83	4.80	−39	20	−7
Right	Frontal	Medial frontal gyrus	0.001	3	6.81	4.79	3	38	38
Left	Sublobar	Insula	0.002	2	6.70	4.74	−39	−19	−1
Right	Limbic	Parahippocampal gyrus	0.002	2	6.68	4.74	27	−1	−13
Right	Sublobar	Claustrum	0.010	1	6.46	4.64	39	−19	−1
Right	Limbic	Anterior Cingulate	0.010	1	6.42	4.63	3	47	2
Left	Frontal	Middle frontal gyrus	0.010	1	6.42	4.63	−48	11	32
Left	Temporal	Superior temporal gyrus	0.010	1	6.30	4.57	−60	−1	5
Left	Parietal	Postcentral gyrus	0.010	1	6.29	4.57	−24	−28	56
Right	Sublobar	Insula	0.010	1	6.22	4.54	33	−25	17
Left	Parietal	Inferior parietal lobule	0.010	1	6.11	4.49	−45	−34	59
Left	Parietal	Postcentral gyrus	0.010	1	6.08	4.48	−60	−22	14
Left	Sublobar	Claustrum	0.010	1	6.01	4.44	−33	−25	8
Left	Sublobar	Insula	0.010	1	6.00	4.44	−33	20	8
Left	Frontal	Precentral gyrus	0.010	1	5.91	4.40	−48	−10	29
Right	Parietal	Postcentral gyrus	0.010	1	5.90	4.39	57	−22	14
Left	Sublobar	Thalamus	0.010	1	5.88	4.39	−15	−16	8
Right	Frontal	Precentral gyrus	0.010	1	5.86	4.38	48	−10	50

FWE, family-wise error. All values in tables derive from the SPM tables.

maximal apnea duration <20 s, ten (47.6%) in the range of 20–30 s, eight (38.1%) in the range of 30–40 s, and one (4.8%) > 40 s. During inspiratory BH, all subjects achieved a maximal apnea duration >20 s, including four (19%) in the range of 20–30 s, six (28.6%) in the range of 30–40 s, and eleven (52.4%) > 40 s.

The mean drop in SpO_2 ± SD was 2.74% ± 2.24 during expiratory BH (range 0.07–7.75) and significantly greater than that observed during inspiratory BH, e.g., 0.93 ± 0.77 (range 0.03–2.63) ($p = 0.0012$). Accordingly, SpO_2 drops of 4% or more were detected in only five subject (24%) who hold their breath for ≥20 s during expiratory BH (be-

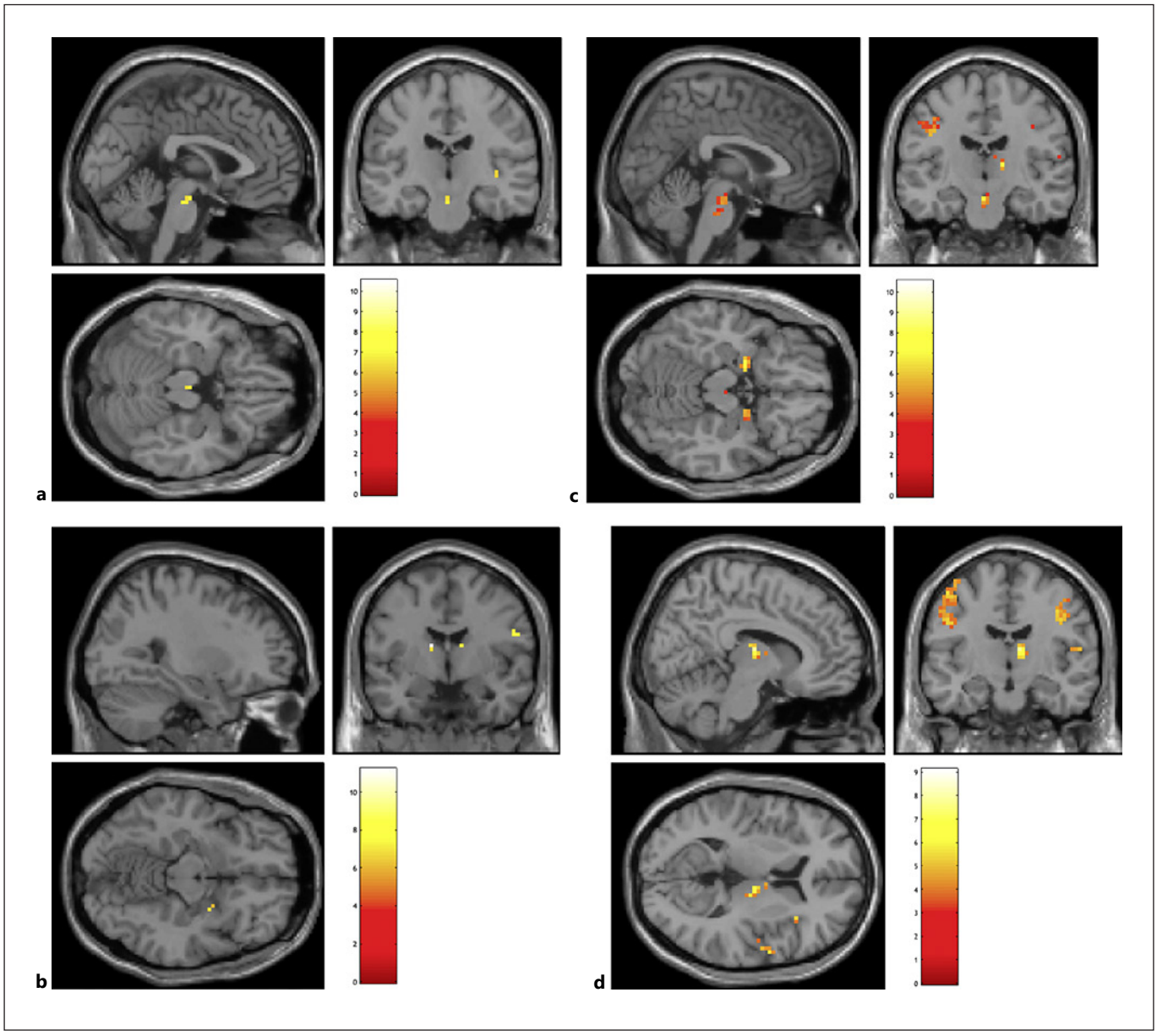

Fig. 2. Group analyses. Expiratory BH (upper row, **a**, **c**) and inspiratory BH (lower row, **b**, **d**). Images obtained using the FWE threshold are shown on the left, while clusters visible using the uncorrected $p = 0.001$ threshold are shown on the right. FWE, family-wise error.

tween 25.1 and 52 s), while such a drop was never observed during inspiratory BH. The drop in SpO_2 positively correlated with the duration of apnea, both during inspiratory ($R = 0.492$, $p = 0.023$) and expiratory BH ($R = 0.679$, $p = 0.001$).

Imaging BOLD Response

Group-Level Analysis

Mask of the brainstem and subcortical/cortical regions (Table 4): During expiratory BH, significant BOLD activation was observed over the pons, the hippocampus and amygdala, the thalamus, the caudate nuclei, and the frontal and temporal cortices (Table 4; Fig. 2a, c). During in-

Table 5. Multivariate analysis of ROI beta values in the brainstem and the thalamus

ROI	Overall effect of expiratory BH	Overall effect of inspiratory BH
Dorsal raphe nucleus	**0.003**	**0.008**
Median raphe	**0.000**	**0.013**
Left ANT of the thalamus	**0.045**	**0.041**
Right ANT of the thalamus	0.617	0.050
Left Kölliker fuse-PB complex	0.085	**0.047**
Right Kölliker fuse-PB complex	0.723	0.453
Left LC	0.235	0.181
Right LC	0.920	0.717
Left lateral reticular nucleus	**0.000**	**0.000**
Right lateral reticular nucleus	**0.010**	**0.005**
Left NA	**0.000**	**0.000**
Right NA	0.182	**0.011**
Left nucleus tractus solitarus	**0.000**	**0.000**
Right nucleus tractus solitarus	**0.014**	**0.000**
Left PBC	**0.000**	**0.000**
Right PBC	0.082	**0.011**
Left ventrolateral thalamus	0.191	0.050
Right ventrolateral thalamus	0.110	**0.013**
Left VRG	**0.000**	**0.000**
Right VRG	0.210	**0.005**

All values in the table represent the *p* values. Bold highlights the significant *p* values.

Table 6. Individual analyses

Condition	Medulla	Pons	Mesencephalon	Hypothalamus	Thalamus	Hippocampus/ amygdala	Brainstem	Brainstem/ hypothalamus
Expiratory BH, *n* (%)	5 (23.8)	17 (80.9)	15 (71.4)	14 (66.6)	15 (71.4)	9 (42.9)	18 (85.7)	19 (90.5)
Inspiratory BH, *n* (%)	1 (4.8)	10 (47.6)	8 (38.1)	12 (57.1)	17 (80.9)	9 (42.9)	12 (57.1)	17 (80.9)
SpO_2 expiratory, *n* (%)	2 (9.5)	4 (19)	3 (14.3)	2 (9.5)	0	4 (19)	5 (23.8)	5 (23.8)
SpO_2 inspiratory, *n* (%)	1 (4.8)	2 (9.5)	3 (14.3)	3 (28.6)	0	6 (28.6)	3 (14.3)	4 (19)

Activations in the brainstem and subcortical structures. Table contains number of subjects per condition and the location of significant clusters.

spiratory BH, similar cortical activations were observed, with additional clusters in the parietal cortex and anterior cingulate, but without significant brainstem activation (Table 4; Fig. 2b, d). However, when directly comparing expiratory and inspiratory BH, no significant difference was evidenced between the two conditions. No significant deactivations were detected.

ROI-Based Analysis

Table 5 details the results from MANOVA analysis using the percentage BOLD change between the task and the baseline obtained from the ROIs located in the brainstem and thalamus. Significant BOLD signal changes were detected in the median and dorsal raphe, left ANT, left NA, left VRG, left lateral reticular nuclei, left pre-Bötzinger complex (PBC), and nucleus tractus solitarus, during both types of BH. Conversely, the right VL nucleus of the thalamus, right PBC, right VRG, right NA, and left Kölliker-Fuse-parabrachial complex were only activated during inspiratory BH. No significant changes were detected in the right ANT, right Kölliker-Fuse-parabrachial complex, LC, and left VL.

Individual Imaging Results

Details about the individual response to the BH within the cortical and subcortical areas involved in respiratory control are provided in Table 6. Nineteen out of the 21 subjects (90.5%) demonstrated a significant response to

Table 7. Individual brainstem BOLD response as a function of apnea duration

Mean duration of apnea	Expiratory BH (Subjects, *n*)	Inspiratory BH (Subjects, *n*)	Brainstem BOLD response during expiratory BH Subjects, *n* (%)	Brainstem BOLD response during inspiratory BH Subjects, *n* (%)
Apnea t <20 s	2	0	2 (100)	0
Apnea 20≤ t ≤30 s	10	4	9 (90)	2 (50)
Apnea 30< t ≤40 s	8	6	7 (87.5)	5 (83.3)
Apnea t >40 s	1	11	1 (100)	5 (45.4)

t (seconds). Indicative values for the relation between apnea duration and significant BOLD activity in the brainstem.

BH at the individual level within the brainstem-hypothalamic area, including 19 during expiratory BH (90.5%), 17 of whom also showed a significant individual response during inspiratory BH (80.9%). These individual responses involved the brainstem proper in 18 subjects (85.7%), including the mesencephalon in 15 (71.4%), the pons in 17 (80.9%), and the medulla in five (23.8%). As a rule, the majority of these responses were observed during both expiratory and inspiratory BH, with slightly more responses for the former. Conversely, thalamic responses, which were present in 17 subjects (80.9%), were more frequent in inspiratory than expiratory BH (i.e., 80.9% vs. 71.4%). All 19 subjects with a significant BOLD response showed activation in some cortical areas (frontal, temporal, parietal, and limbic regions). Online supplementary Figure 1 (for all online suppl. material, see www.karger.com/doi/10.1159/000529388) shows examples of individual BOLD activations in two subjects for the two BH tasks.

Of note, one of the only two subjects in whom the BOLD signal did not significantly vary is a professional athlete (mean variation of SpO2 1.062%), while the second subject suffered significant variations in performance across BH sessions (from 11 to 27 s for expiratory BH and 22–38 s for inspiratory BH). Deactivations within the brainstem were also observed in eight subjects during inspiratory BH, and ten subjects during expiratory BHs.

Adjusting individual analyses to changes in SpO_2 did not improve their sensitivity with less subjects showing significant BOLD activation. Yet, all five subjects with a drop in SPO_2 ≥4% displayed a significant BOLD response in the medulla and the pons.

The duration of expiratory BH did not seem to influence the likelihood of significant individual response, with comparable findings for all ranges of apnea duration (Table 7). In contrast, the duration of inspiratory BH might have an impact on the proportion of significant BOLD activation, with 83% of subjects performing an apnea of 30 < t ≤40 s showing such an activation, as compared to only 45–50% for shorter or longer apnea (Table 7). Yet, this difference was not statistically tested according to the small number of subjects in each category.

Individual versus Group Comparison

No subject showed a significant difference in BOLD activation maps when compared to the group of all other subjects, including the two subjects who failed to demonstrate a significant fMRI activation during BH.

Discussion

The primary goal of the present human fMRI study was to trigger an activation of the respiratory centers that would prove assessable at the individual patient level, using a simple BH paradigm easily implementable in clinical routine. This would open the door to the development of a clinically relevant biomarker for conditions with a suspected dysfunction of central respiratory control. We observed a significant BOLD response in the brainstem and hypothalamus in 90.5% of our normal subjects, with one of the only two exceptions observed in a professional athlete and the other in a subject with unreliable BH. Furthermore, none of our control subjects showed a significant difference when tested against the group of all other controls. These findings are encouraging toward the possibility of using this simple paradigm in relevant patients with the hope to delineate significant abnormalities at the individual level.

The BH paradigm with unconstrained duration is characterized by very heterogeneous duration of apnea and associated levels of SpO_2 [27, 31, 38], as observed in our study. Yet, despite variation in BH duration, the BOLD signal can be robustly mapped [27]. As previously reported, inspiratory BH was significantly longer than expiratory BH while associated with milder reduction in

SpO_2 [24], with a positive correlation between the duration of apneas and the drop of SpO_2, regardless of the type of BH [39]. Our subjects were requested to hold their breath as long as it was bearable, leading the majority to execute expiratory BH lasting between 20 and 30 s and to show a BOLD response, regardless of the duration of expiratory BH. For inspiratory BH, the proportion of significant BOLD response was observed in 83% of participants that performed 30–40 s BH but in only half of those who performed inspiratory BH of shorter or longer duration. Previous reports suggested that apnea duration of 20 s is required to obtain a reliable BOLD response for expiratory BH [27] and more than 20 s for inspiratory BH [40]. While our findings are consistent with these observations for expiratory BH, they suggest that longer inspiratory BH, between 30 and 40 s, is associated with a greater likelihood of a BOLD response within the brainstem. Interestingly, we also found that drops of SpO_2 of more than 4% systematically led to a strong individual response from VRG and PRG.

Mechanisms regulating the individual duration of BH remain uncertain [41, 42]. The act of holding one's breath engages a conscious inhibitory stimulus which is eventually overwhelmed by an involuntary stimulus, forcing the subject to finally inspire or expire [43, 44]. The centers that are responsive for the urge to breathe are located in the medulla oblongata and include serotoninergic neurons that detect increased pCO_2 and then fire to stimulate respiration [45, 46]. Their reactivity to the hypercapnic condition seems to vary greatly [2], and the difference in BOLD response to hypercapnia might be due to difference in neuronal activation of these centers [47]. Animal studies [9, 48–52] also helped define the role and associations of structures involved in the semiology of breathing. These studies highlight the essential connections of the thalamus with the supplementary motor area, premotor, frontal, prefrontal, and anterior-cingulate cortex, and the anterior insula. In particular, the thalamocortical serotoninergic projections induce cortical arousal, mediating the "life-saving" response to hypercapnia [45]. The hypothalamus also plays an essential role in hypoxic and hypercapnic conditions [53].

Our group-level analyses showed BH-triggered activation in the majority of regions known to participate in the central regulation of breathing, i.e., the PRG, medial and dorsal raphe nuclei, thalamus, caudate, hippocampus, and cortical areas located in the frontal, parietal, and temporal lobes. When extracting signal from predefined ROIs centered around known respiratory centers, fMRI responses to both expiratory and inspiratory BH were observed over the median and dorsal raphe, thalamus, the DRG, the PBC complex, and the VRG. At the individual level, BOLD activation in both types of BH was observed in cortical areas (frontal, parietal, temporal, and limbic regions), the diencephalon, the mesencephalon, the apneustic and the pneumotaxic centers, the ventral-lateral pons, as well as the DRG, the VRG, and the raphe nuclei. These results are consistent with previous studies which described regions susceptible to hypercapnic challenges [54, 55] and BH [31]. These regions are typically well irrigated and associated with high BOLD sensitivity [56]. Several of these respiratory centers, such as the DRG and inferior ventral pons, the NA, and PBC [2], are also composed of chemo-sensitive and rhythm generator cells [57] which, when activated, reflect the direct impact of hypercapnia and the increase in respiratory motor activity [2].

Numerical differences were observed between expiratory and inspiratory BH using voxel-based SPM analyses, with more brainstem activation during expiratory BH, in particular within the pons, and more cortical activation during inspiratory BH, in particular within the anterior cingulate. These differences did not prove significant, however, possibly due to the limited sample size of our cohort. Few other fMRI studies have investigated the human brainstem in the autonomic or voluntary control of breathing using different methods [2, 13, 26]. Some resting-state fMRI studies aimed at quantifying the noise contribution to the resting BOLD signal, particularly in the brainstem [26, 58]. While quantifying the BOLD response in the brainstem is fairly challenging, it can be reliably quantified if appropriate correction for noise, motion, cardiac and respiratory activities, and end-tidal CO2 is applied [26, 58]. An fMRI study using inhalation of CO_2 in 12 healthy volunteers showed changes in BOLD signal in dorsal rostral pons, the inferior ventral pons, and the dorsal and lateral medulla [2]. Another study compared the whole-brain activation during BH to activation after CO_2 administration challenge in order to delineate the nonspecific whole-brain activation (vasodilatory effect of CO_2) from the local neural-related BOLD signal change [13]. Similar to our study, they found a response to BH in six healthy volunteers over cortical and subcortical structures including the insula, basal ganglia, frontal cortex, parietal cortex and thalamus, and the pons.

In about half of our subjects, we detected simultaneous activation of the limbic structures – amygdala and/or hippocampus during BH. Recent data from direct electrical cortical stimulation experiments suggest that

the human amygdalohippocampal complex can exert effects on breathing [34, 59] and might play a crucial role in patients with epilepsy who are at risk of SUDEP [60].

To our knowledge, only one other study provided results of BH-triggered fMRI response at the individual level in six healthy subjects [13]. While most subjects in that study showed significant fMRI activations following inspiratory BH, in particular over the dorsal somatosensory cortex, the cerebellum, and the cingulate gyrus, bilaterally, a large heterogeneity of BOLD activation was observed across individuals. Another study used CO_2 challenge in healthy volunteers to trigger central hypercapnic response [47]. Individual maps demonstrated BOLD responses in the cortex, the thalamus, the pons, and the medulla, similar to those reported in our study [47].

BOLD signal failed to be significant in two of our 21 subjects, likely due in one subject to his athletic performances and tolerance to long-lasting apnea, while the second subject was not compliant with the BH challenges. Experimental procedures ought to be considered carefully and conducted properly for triggering the respiratory centers. The critical steps within our protocol included implementing a respiration-triggered paradigm to allow subjects to be comfortable enough to comply with the task. Confounding variables such as habituation, anxiety within the scanner, and respiration patterns in different people need to be considered when designing a paradigm and analyzing the data. Poor compliance to even one BH will affect the recorded time series [31]. The fMRI data are generally highly variable between subjects and even within one subject, and for repetitive or demanding tasks as our BH maneuver, cooperation of the subject is necessary. While BH is fairly easy to implement using a visual cue, noncompliancy might represent an issue in some populations (e.g., patients with cognitive disorders, elderlies, children).

BH task or CO_2 inhalation-induced hypercapnia have both been used to evaluate cerebrovascular reactivity in various diseases [61, 62]. BH fMRI has also been used to explore the brain activation patterns in OSA, bipolar disorders, acute stroke, and gliomas [63–66]. In patients with OSA, overall cortical and brainstem activation patterns were significantly reduced compared to healthy controls [63]. Additionally, researchers found positive correlations between resting state and cerebrovascular reactivity following the BH task in elderly [67] and slower BOLD responses in Alzheimer disease following CO_2 challenge [68]. Based on our findings, we believe that BH-triggered fMRI could be further used in other patient populations to investigate disorders of central respiratory regulation, in particular in patients with central hypoventilation syndrome, central sleep apnea, sudden infant death syndrome, or syndrome Prader-Willi and those with epilepsy at risk of SUDEP. Indeed, SUDEP has been found to be primarily derived from postictal seizure-triggered central respiratory arrest, suggesting an altered response of the brainstem respiratory centers to hypoxia [69]. We are currently running such a study in persons with epilepsy.

Various limitations should be addressed. First, because we chose to sample the BOLD signal from the entire brain, we chose a larger field of view and a high TR (2,520 ms) that limited the sampling rate of cardiac and respiratory cycles which could have affected the time series [56]. Second, the accuracy in measurements of airflow and exhaled gas pressures may have been altered by the use of the mask without use of a nose clip [12]. Due to logistical capacity, we could not use both instruments. However, the use of a thoracic belt allowed us to visualize the thoracic movement, which, associated with the absence of gas exchanges in the mask (pCO_2 and pO_2), delineated the apnea period. Finally, the brainstem is a complex structure that is difficult to precisely differentiate in fMRI imaging due to its low spatial resolution. Accordingly, we considered BOLD activity in the mesencephalon as reflecting the anatomical location of the raphe nuclei and clusters in PRG as reflecting the activation of the Kölliker-Fuse/parabrachial complex, LC, and apneustic center. Signal in the VRG was considered to reflect the activity in the parafacial nucleus, Bötzinger, PBC, cVRG, and rVRG.

Conclusion

BH maneuver is an effective and easy to implement trigger of central respiratory centers which provide robust fMRI response in humans at the individual level and could prove to be a useful biomarker in various medical conditions associated with central respiratory dysfunction.

Acknowledgments

We thank all subjects that took part in this research. We would also like to thank the medical and technical staff at LREN, CHUV for assistance and technical support.

Statement of Ethics

This study protocol was reviewed and approved by Ethical committee of Canton de Vaud, approval 2016-02057. All subjects gave written informed consent to participate in this study.

Conflict of Interest Statement

Authors declare no conflict of interest.

Funding Sources

The study was supported by two grants from InnoCentive Challenges – The SUDEP Institute Challenge: Developing Predictive Biomarkers of Epilepsy Seizures.

Author Contributions

CC, MB, and PR wrote the manuscript and performed the statistical analysis. RB developed the in-house software to mark the BH. SR, JH, and SL participated in the design, statistical analysis, and proof-reading. DI was responsible for the design of the technical part of the experiment, from behavioral testing to MR scanning.

Data Availability Statement

All data generated or analyzed during this study are included in this article and its online supplementary material. Further inquiries can be directed to the corresponding author.

References

1 Rybak IA, O'Connor R, Ross A, Shevtsova NA, Nuding SC, Segers LS, et al. Reconfiguration of the pontomedullary respiratory network: a computational modeling study with coordinated in vivo experiments. J Neurophysiol. 2008;100(4):1770–99.
2 Pattinson KT, Mitsis GD, Harvey AK, Jbabdi S, Dirckx S, Mayhew SD, et al. Determination of the human brainstem respiratory control network and its cortical connections in vivo using functional and structural imaging. Neuroimage. 2009 Jan 15;44(2):295–305.
3 Lundblad LC, Fatouleh RH, Hammam E, McKenzie DK, Macefield VG, Henderson LA. Brainstem changes associated with increased muscle sympathetic drive in obstructive sleep apnoea. NeuroImage. 2014;103:258–66.
4 Devinsky O, Hesdorffer DC, Thurman DJ, Lhatoo SD, Richerson GB. Sudden unexpected death in epilepsy: epidemiology, mechanisms, and prevention. Lancet Neurol. 2016;15(10):1075–88.
5 Lavezzi AM, Ottaviani G, Rossi L, Matturri L. Cytoarchitectural organization of the parabrachial/Kölliker-Fuse complex in manlliker-Fuse complex in man. Brain Dev. 2004;26(5):316–20.
6 Trang H. Les pathologies du contrôle respiratoire chez l'enfant. Medecine du Sommeil. 2005;2(6):13–7.
7 Patwari PP, Carroll MS, Rand CM, Kumar R, Harper R, Weese-Mayer DE. Congenital central hypoventilation syndrome and the PHOX2B gene: a model of respiratory and autonomic dysregulation. Respir Physiol Neurobiol. 2010;173(3):322–35.
8 Guyenet PG, Mulkey DK. Retrotrapezoid nucleus and parafacial respiratory group. Respir Physiol Neurobiol. 2010;173(3):244–55.
9 Smith JC, Abdala APL, Borgmann A, Rybak IA, Paton JF. Brainstem respiratory networks: building blocks and microcircuits. Trends Neurosci. 2013;36(3):152–62.
10 Zoccal DB, Silva JN, Barnett WH, Lemes EV, Falquetto B, Colombari E, et al. Interaction between the retrotrapezoid nucleus and the parafacial respiratory group to regulate active expiration and sympathetic activity in rats. Am J Physiol Lung Cell Mol Physiol. 2018;315(5):L891–909.
11 Smith JC, Ellenberger HH, Ballanyi K, Richter DW, Feldman JL. Pre-Botzinger complex: a brainstem region that may generate respiratory rhythm in mammals. Science. 1991 Nov 1;254(5032):726–9.
12 McKay LC, Evans KC, Frackowiak RSJ, Corfield DR. Neural correlates of voluntary breathing in humans. J Appl Physiol. 2003;95(3):1170–8.
13 McKay LC, Adams L, Frackowiak RS, Corfield DR. A bilateral cortico-bulbar network associated with breath holding in humans, determined by functional magnetic resonance imaging. NeuroImage. 2008;40(4):1824–32.
14 Kastrup A, Li TQ, Takahashi A, Glover GH, Moseley ME. Functional magnetic resonance imaging of regional cerebral blood oxygenation changes during breath holding. Stroke. 1998 Dec;29(12):2641–5.
15 Li TQ, Kastrup A, Takahashi AM, Moseley ME. Functional MRI of human brain during breath holding by BOLD and FAIR techniques. Neuroimage. 1999 Feb;9(2):243–9.
16 Thomason ME, Burrows BE, Gabrieli JD, Glover GH. Breath holding reveals differences in fMRI BOLD signal in children and adults. Neuroimage. 2005 Apr 15;25(3):824–37.
17 Pinto J, Bright MG, Bulte DP, Figueiredo P. Cerebrovascular reactivity mapping without gas challenges: a methodological guide. Front Physiol. 2021;11:608475.
18 Chen K, Yang H, Zhang H, Meng C, Becker B, Biswal B. Altered cerebrovascular reactivity due to respiratory rate and breath holding: a BOLD-fMRI study on healthy adults. Brain Struct Funct. 2021 May;226(4):1229–39.
19 Pattinson KT, Governo RJ, MacIntosh BJ, Russell EC, Corfield DR, Tracey I, et al. Opioids depress cortical centers responsible for the volitional control of respiration. J Neurosci. 2009 Jun 24;29(25):8177–86.
20 Ciumas C, Rheims S, Ryvlin P. fMRI studies evaluating central respiratory control in humans. Front Neural Circuits. 2022;16:982963.
21 Thomason ME, Glover GH. Controlled inspiration depth reduces variance in breath-holding induced BOLD signal. NeuroImage. 2008;39(1):206–14.
22 Beissner F, Schumann A, Brunn F, Eisenträger D, Bär KJ. Advances in functional magnetic resonance imaging of the human brainstem. NeuroImage. 2014;86:91–8.
23 Ishiwata T, Tsushima K, Fujie M, Suzuki K, Hirota K, Abe M, et al. End-tidal capnographic monitoring to detect apnea episodes during flexible bronchoscopy under sedation. BMC Pulm Med. 2017;17(1):17.
24 Urback AL, MacIntosh BJ, Goldstein BI. Cerebrovascular reactivity measured by functional magnetic resonance imaging during breath-hold challenge: a systematic review. Neurosci Biobehav Rev. 2017;79:27–47.
25 Birn RM, Smith MA, Jones TB, Bandettini PA. The Respiration response function: the temporal dynamics of fMRI signal fluctuations related to changes in respiration. Neuroimage. 2008;40(2):644–54.
26 Harvey AK, Pattinson KT, Brooks JC, Mayhew SD, Jenkinson M, Wise RG. Brainstem functional magnetic resonance imaging: disentangling signal from physiological noise. J Magn Reson Imaging. 2008;28(6):1337–44.
27 Bright MG, Murphy K. Reliable quantification of BOLD fMRI cerebrovascular reactivity despite poor breath-hold performance. NeuroImage. 2013;83:559–68.

28 Friese S, Hamhaber U, Erb M, Kueker W, Klose U. The influence of pulse and respiration on spinal cerebrospinal fluid pulsation. Invest Radiol. 2004;39(2):120–30.
29 Tancredi FB, Hoge RD. Comparison of cerebral vascular reactivity measures obtained using breath-holding and CO2 inhalation. J Cereb Blood Flow Metab. 2013;33(7):1066–74.
30 Caballero-Gaudes C, Reynolds RC. Methods for cleaning the BOLD fMRI signal. NeuroImage. 2017;154:128–49.
31 Murphy K, Harris AD, Wise RG. Robustly measuring vascular reactivity differences with breath-hold: normalising stimulus-evoked and resting state BOLD fMRI data. Neuroimage. 2011 Jan 1;54(1):369–79.
32 Glover GH, Li TQ, Ress D. Image-based method for retrospective correction of physiological motion effects in fMRI: retroicor. Magn Reson Med. 2000;44(1):162–7.
33 Evans KC. Cortico-limbic circuitry and the airways: insights from functional neuroimaging of respiratory afferents and efferents. Biol Psychol. 2010;84(1):13–25.
34 Lacuey N, Zonjy B, Londono L, Lhatoo SD. Amygdala and hippocampus are symptomatogenic zones for central apneic seizures. Neurology. 2017 Feb 14;88(7):701–5.
35 Marincovich A, Bravo E, Dlouhy B, Richerson GB Amygdala lesions reduce seizure-induced respiratory arrest in DBA/1 mice. Epilepsy Behavior. 2021;121:106440.
36 Fink GR, Corfield DR, Murphy K, Kobayashi I, Dettmers C, Adams L, et al. Human cerebral activity with increasing inspiratory force: a study using positron emission tomography. J Appl Physiol (1985). 1996;81(3):1295–305.
37 Banzett RB, Garcia RT, Moosavi SH. Simple contrivance "clamps" end-tidal PCO(2) and PO(2) despite rapid changes in ventilation. J Appl Physiol (1985). 2000;88(5):1597–600.
38 Sutterlin S, Schroijen M, Constantinou E, Smets E, Van den Bergh O, Van Diest I. Breath holding duration as a measure of distress tolerance: examining its relation to measures of executive control. Front Psychol. 2013;4:483.
39 Strohl KP, Altose MD. Oxygen saturation during breath-holding and during apneas in sleep. Chest. 1984;85(2):181–6.
40 Magon S, Basso G, Farace P, Ricciardi GK, Beltramello A, Sbarbati A. Reproducibility of BOLD signal change induced by breath holding. Neuroimage. 2009 Apr 15;45(3):702–12.
41 Godfrey S, Campbell EJ. The control of breath holding. Respir Physiol. 1968;5(3):385–400.
42 Breskovic T, Lojpur M, Maslov PZ, Cross TJ, Kraljevic J, Ljubkovic M, et al. The influence of varying inspired fractions of O2 and CO2 on the development of involuntary breathing movements during maximal apnoea. Respir Physiol Neurobiol. 2012;181(2):228–33.
43 Parkes MJ. Breath-holding and its breakpoint. Exp Physiol. 2006;91(1):1–15.
44 Vassilakopoulos T. Chapter 6-control of ventilation and respiratory muscles. In: Spiro SG, Silvestri GA, Agustí A, editors. Clinical respiratory medicine. 4th ed. Philadelphia: W.B. Saunders; 2012. p. 50–62.
45 Buchanan GF, Richerson GB. Central serotonin neurons are required for arousal to CO2. Proc Natl Acad Sci U S A. 2010;107(37):16354–9.
46 Guyenet PG, Bayliss DA. Neural control of breathing and CO2 homeostasis. Neuron. 2015;87(5):946–61.
47 Prokopiou PC, Pattinson KTS, Wise RG, Mitsis GD. Modeling of dynamic cerebrovascular reactivity to spontaneous and externally induced CO2 fluctuations in the human brain using BOLD-fMRI. Neuroimage. 2019 Feb 1;186:533–48.
48 Bianchi AL, Denavit-Saubie M, Champagnat J. Central control of breathing in mammals: neuronal circuitry, membrane properties, and neurotransmitters. Physiol Rev. 1995;75(1):1–45.
49 Kannurpatti SS, Biswal BB, Hudetz AG. Differential fMRI-BOLD signal response to apnea in humans and anesthetized rats. Magn Reson Med. 2002;47(5):864–70.
50 St-John WM, Paton JF. Role of pontile mechanisms in the neurogenesis of eupnea. Respir Physiol Neurobiol. 2004;143(2–3):321–32.
51 Rosin DL, Chang DA, Guyenet PG. Afferent and efferent connections of the rat retrotrapezoid nucleus. J Comp Neurol. 2006;499(1):64–89.
52 Zerweck L, Hauser TK, Roder C, Klose U. Investigation of the BOLD-based MRI signal time course during short breath-hold periods for estimation of the cerebrovascular reactivity. SN Compr Clin Med. 2020;2(9):1551–62.
53 Fukushi I, Yokota S, Okada Y. The role of the hypothalamus in modulation of respiration. Respir Physiol Neurobiol. 2019 Jul;265:172–9.
54 Rostrup E, Law I, Blinkenberg M, Larsson HB, Born AP, Holm S, et al. Regional differences in the CBF and BOLD responses to hypercapnia: a combined PET and fMRI study. Neuroimage. 2000 Feb;11(2):87–97.
55 Tancredi FB, Gauthier CJ, Madjar C, Bolar DS, Fisher JA, Wang DJ, et al. Comparison of pulsed and pseudocontinuous arterial spin-labeling for measuring CO2 -induced cerebrovascular reactivity. J Magn Reson Imaging. 2012 Aug;36(2):312–21.
56 Golestani AM, Chang C, Kwinta JB, Khatamian YB, Jean Chen J. Mapping the end-tidal CO2 response function in the resting-state BOLD fMRI signal: spatial specificity, test–retest reliability and effect of fMRI sampling rate. NeuroImage. 2015;104:266–77.
57 Feldman JL, Del Negro CA. Looking for inspiration: new perspectives on respiratory rhythm. Nat Rev Neurosci. 2006;7(3):232–42.
58 Harita S, Stroman PW. Confirmation of resting-state BOLD fluctuations in the human brainstem and spinal cord after identification and removal of physiological noise. Magn Reson Med. 2017 Dec;78(6):2149–56.
59 Nobis WP, Schuele S, Templer JW, Zhou G, Lane G, Rosenow JM, et al. Amygdala-stimulation-induced apnea is attention and nasal-breathing dependent. Ann Neurol. 2018 Mar;83(3):460–71.
60 Lacuey N, Hampson JP, Harper RM, Miller JP, Lhatoo S. Limbic and paralimbic structures driving ictal central apnea. Neurology. 2019 Feb 12;92(7):e655–69.
61 Spano VR, Mandell DM, Poublanc J, Sam K, Battisti-Charbonney A, Pucci O, et al. CO2 blood oxygen level-dependent MR mapping of cerebrovascular reserve in a clinical population: safety, tolerability, and technical feasibility. Radiology. 2013 Feb;266(2):592–8.
62 Liu P, De Vis JB, Lu H. Cerebrovascular reactivity (CVR) MRI with CO2 challenge: a technical review. Neuroimage. 2019 Feb 15;187:104–15.
63 Buterbaugh J, Wynstra C, Provencio N, Combs D, Gilbert M, Parthasarathy S. Cerebrovascular reactivity in young subjects with sleep apnea. Sleep. 2015;38(2):241–50.
64 Iranmahboob A, Peck KK, Brennan NP, Karimi S, Fisicaro R, Hou B, et al. Vascular reactivity maps in patients with gliomas using breath-holding BOLD fMRI. J Neuroimaging. 2016;26(2):232–9.
65 Raut RV, Nair VA, Sattin JA, Prabhakaran V. Hypercapnic evaluation of vascular reactivity in healthy aging and acute stroke via functional MRI. Neuroimage Clin. 2016;12:173–9.
66 Urback AL, Metcalfe AW, Korczak DJ, MacIntosh BJ, Goldstein BI. Reduced cerebrovascular reactivity among adolescents with bipolar disorder. Bipolar Disord. 2019;21(2):124–31.
67 Jahanian H, Christen T, Moseley ME, Pajewski NM, Wright CB, Tamura MK, et al. Measuring vascular reactivity with resting-state blood oxygenation level-dependent (BOLD) signal fluctuations: a potential alternative to the breath-holding challenge? J Cereb Blood Flow Metab. 2017;37(7):2526–38.
68 Richiardi J, Monsch AU, Haas T, Barkhof F, Van de Ville D, Radu EW, et al. Altered cerebrovascular reactivity velocity in mild cognitive impairment and Alzheimer's disease. Neurobiol Aging. 2015 Jan;36(1):33–41.
69 Ryvlin P, Nashef L, Lhatoo SD, Bateman LM, Bird J, Bleasel A, et al. Incidence and mechanisms of cardiorespiratory arrests in epilepsy monitoring units (MORTEMUS): a retrospective study. Lancet Neurol. 2013 Oct;12(10):966–77.